Optical evaluation of antioxidant activity: a comparison between a spectrophotometer and a homebuilt photometer.

Pitcha Luengviriya[1], *Kornkamon* Kiatsommart[1], *Chanida* Leelakanok[1], *Supanun* Patumorathai[1], *Kwanruthai* Sibsiri[2], and *Thidarat* Wangkham[3*]

[1]Mahidol University International Demonstration School, Salaya, Phuttamonthon, 73170 Nakhon Pathom, Thailand
[2]Department of Physics, Kasetsart University, Jatujak, 10900 Bangkok, Thailand
[3]Biomedical Engineering program, Department of Industrial Physics and Medical Instrumentation, Lasers and Optics Research Center, King Mongkut's University of Technology North Bangkok, Wongsawang, Bangsue, 10800 Bangkok, Thailand

Abstract. The antioxidant activity of an orange peel extract is determined using a DPPH (2,2-diphenyl-1-picrylhydrazyl) solution. Sample absorption is measured with both a commercial spectrophotometer and a homebuilt photometer equipped with a 525-nm LED. Small, dried pieces of orange peel are extracted using 95% ethanol. Seven DPPH solutions with concentrations ranging from 0.1 to 0.4 mM are measured to establish calibration equations. For the spectrophotometer, absorbance exhibits a linear increase with DPPH concentration at both 517 nm (absorbance peak) and 525 nm (matching the LED in the photometer). In the homebuilt photometer, three piecewise linear fittings for concentration 0.1– 0.4 mM provide a better representation of absorption data compared to a single overall fitting across 0.1–0.4 mM. Different volumes of orange peel extract are added into the DPPH solution (0.4 mM DPPH after mixing) and stored in darkness for 30 minutes before the measurement. In both spectrophotometer and photometer analyses, antioxidant activity increases with the extract volume. Using spectrophotometer measurements as reference, the photometer with piecewise fittings produces significantly lower errors compared to those obtained with overall fitting.

1 Introduction

Free radicals are highly reactive molecules that can lead to oxidative damage to biological systems, leading to cell aging and various diseases, such as inflammation, neurodegenerative disorders, cardiovascular diseases, and cancer [1, 2]. These reactive species are generated by endogenous metabolic processes and environmental factors like pollution, radiation, and unhealthy diets [3, 4]. Over time, excessive oxidative stress can overwhelm the body's natural defense mechanisms, resulting in cellular dysfunction and disease progression [5]. Recent studies indicate that oxidative stress is not only a consequence of external environmental factors but is also closely linked to metabolic disorders such as diabetes and obesity, emphasizing the need for effective antioxidant strategies to mitigate these effects [6].

Antioxidants are key agents in neutralizing free radicals and reducing oxidative harm, thereby protecting cells from premature aging and disease development [7, 8]. These protective compounds are found in a variety of food sources, including fruits, vegetables, and medicinal plants, and have been extensively studied in food science, medicine, and nutrition research [9, 10]. Researchers are exploring bioactive compounds from natural sources, including marine algae, fungi, and novel plant extracts, as potential therapeutic antioxidants for combating oxidative stress-related disorders [11-13].

The ability to assess antioxidant activity accurately is essential for understanding their potential benefits and applications in health and disease prevention [14, 15]. One widely used method for evaluating antioxidant activity is the DPPH (2, 2-diphenyl-1-picrylhydrazyl) assay. This technique relies on the scavenging ability of antioxidants to reduce the DPPH radical, causing a measurable color change [16, 17]. The reaction is quantified using spectrophotometry, a reliable and well-established technique for determining antioxidant potency [18].

Although commercial spectrophotometers provide precise results, they can be expensive and require laboratory infrastructure, which may limit accessibility for some researchers and institutions [19-21]. Recent advancements have led to the development of cost-effective, homebuilt optical devices, such as photometers utilizing LED technology. These alternative devices offer an affordable solution for antioxidant measurement, making this research more accessible to broader scientific communities [22, 23]. Studies have demonstrated that such homemade optical tools can effectively quantify antioxidant activity with reasonable accuracy, presenting a viable alternative to traditional spectrophotometry.

* Corresponding author: thidarat.w@sci.kmutnb.ac.th

Innovations in smartphone-integrated optical sensors are emerging as promising tools for real-time antioxidant analysis, further expanding accessibility [24, 25]. Current developments include wearable sensors capable of detecting oxidative stress biomarkers, which could facilitate early disease diagnosis and personalized health monitoring [26].

Natural products, including citrus fruits, are sources of antioxidants. Orange peels contain bioactive compounds, which are flavonoids, carotenoids, and phenolic acids, exhibit strong radical-scavenging properties [27, 28]. Investigating the antioxidant activity of orange peel extracts can provide insights into their potential health benefits and applications in food science and nutraceuticals [29]. Beyond dietary applications, orange peel antioxidants are also being explored for their use in skincare, cosmetics, and biodegradable packaging materials due to their antimicrobial and preservative properties, highlighting their multifunctional potential [30-32].

In this article, we present a comparative study evaluating a commercial spectrophotometer and a homebuilt LED-based photometer for measuring the antioxidant activity of orange peel extract. By testing various concentrations and wavelengths, we assess whether a low-cost optical device can serve as an effective alternative to traditional spectrophotometric methods.

2 Methods

2.1 Preparation of DPPH Stock Solution

A stock solution of 100 mL DPPH (2, 2-diphenyl-1-picrylhydrazyl) with a concentration of 1 mM in 95% ethanol is prepared as follows. The required amount of DPPH powder is calculated based on its molecular weight (394.32 g/mol), yielding approximately 39.43 mg of DPPH for the solution. Using a high-precision balance, this amount is carefully weighed to ensure accuracy. The weighed DPPH is then transferred into a clean 100-mL volumetric flask, followed by gradual addition of 95% ethanol with continuous gentle stirring to facilitate complete dissolution.

Once fully dissolved, the solution volume is adjusted to 100 mL using the same solvent. To prevent degradation due to light exposure, the container is wrapped in aluminum foil and stored at 4°C in a refrigerator. The solution is allowed to reach room temperature before use to ensure consistency in measurements.

2.2 Preparation of Diluted DPPH Solutions

To study the relationship between absorbance and concentration, a set of seven diluted DPPH solutions is prepared with concentrations of 0.10, 0.15, 0.20, 0.25, 0.30, 0.35, and 0.40 mM in 95% ethanol. These solutions are obtained by precisely diluting the stock solution in clean volumetric flasks, ensuring uniform mixing. Each dilution step is carried out using calibrated micropipettes for accuracy.

2.3 Preparation of Orange Peel Extract

The extraction of orange peel antioxidants begins with thoroughly washing fresh orange peels under running tap water to remove any dirt or contaminants. The cleaned peels are then cut into small uniform pieces and dried in a well-ventilated dry area for approximately one week, ensuring complete moisture removal.

Following the drying step, 5 grams of completely dried orange peel pieces are accurately weighed using an analytical balance. These pieces are then placed in a 50-mL extraction bottle and extracted using 25 mL of 95% ethanol. The extraction process is carried out over 24 hours at room temperature, ensuring efficient diffusion of bioactive compounds into the solvent. After extraction, the liquid phase is separated from solid residues through filtration using Whatman filter paper and is then stored at 4°C for subsequent analysis.

2.4 Spectrophotometric Analysis

The absorbance measurements of the DPPH solutions and orange peel extract are conducted using LAMBDA 365 UV/Vis spectrophotometer (Perkin Elmer). Each sample solution is placed into 1-cm spectrophotometric quartz cells to minimize optical interference.

The absorbance spectra of the DPPH solutions are investigated across a wavelength range of 400–700 nm. The primary absorbance peak occurs at 517 nm, which is commonly used for antioxidant evaluation. Additionally, measurements at 525 nm are performed to match the LED source in the homebuilt photometer.

Using the absorbance values obtained, linear calibration equations are constructed to establish the relationship between absorbance (x) and concentration (y), expressed as:

$$y = a\,x + b \qquad (1)$$

where a and b are coefficients determined from experimental data.

2.5 Homebuilt Photometer Operation

Our homebuilt photometer is designed to provide a cost-effective and accessible method for measuring antioxidant activity. It consists of an Arduino Uno microcontroller board, a 525-nm LED light source, a light-dependent resistor (LDR) detector, and an LCD monitor for displaying the results.

The 525-nm LED is the primary illumination source for the photometric measurements. To ensure stable and adjustable light intensity, the LED is controlled using pulse-width modulation (PWM), which allows precise regulation of brightness. The LED is connected in series with a resistor and capacitor to stabilize the voltage and prevent fluctuations during operation. The PWM signal, generated from the Arduino Uno, modulates the duty cycle of the LED, controlling the brightness dynamically depending on the required intensity.

The transmitted light passing through the 1-cm spectrophotometric cuvette containing the sample

solution is detected by the LDR sensor. The LDR is incorporated into a voltage-divider circuit, where it is connected in series with a fixed resistor and powered by a 5V DC supply. The voltage across the LDR changes proportionally to the light intensity it receives—higher illumination results in lower resistance, leading to higher voltage readings.

The Arduino Uno board reads the voltage signal from the LDR sensor and performs an analog-to-digital (A/D) conversion with a 10-bit resolution (1024 levels) over a 0–5V range. The resulting digitized voltage (v) represents the detected light intensity and is displayed on an LCD screen for real-time monitoring. To ensure accurate measurements, background noise and fluctuations are minimized by shielding external light interference.

To eliminate errors caused by variations in initial light intensity, a blank measurement is conducted using 95% ethanol solution before each DPPH test. The corresponding blank voltage (v_0) is recorded, and the absorption (Δv) is determined by calculating the difference between blank and sample voltage: $\Delta v = v_0 - v$. This difference represents the absorption and is used for constructing a calibration equation describing the linear relationship between absorption and concentration (y):

$$y = a\,\Delta v + b \qquad (2)$$

where a and b are calibration coefficients determined experimentally.

2.6 Antioxidant Activity Measurement

The antioxidant activity of orange peel extract is evaluated at varying concentrations using a DPPH assay. A total of four test tubes are prepared, each containing 2 mL of 0.60 mM DPPH solution. The orange peel extract is then added in precise volumes of 0, 0.2, 0.4, and 0.6 mL, respectively. To ensure that the final volume remains consistent at 3 mL and that the initial DPPH concentration is uniformly adjusted to 0.40 mM, 95% ethanol is used to make up the remaining volume in each tube.

To prevent degradation due to light exposure, the prepared test tubes are covered with aluminum foil and kept in darkness for 30 minutes to allow the reaction between DPPH and antioxidant compounds to stabilize before absorption measurements.

After incubation, the DPPH-extract mixtures are carefully transferred into 1-cm spectrophotometric quartz cells to minimize external optical interference. The absorption of each sample is measured using both the UV/Vis spectrophotometer and the homebuilt photometer, providing comparative results.

For measurements using a LAMBDA 365 UV/Vis spectrophotometer, the antioxidant activity (AA%) is calculated based on the absorbance values of solutions without and with the orange peel extract using the equation:

$$AA(\%) = \frac{x_{ref} - x_{ext}}{x_{ref}} \times 100\% \qquad (3)$$

where x_{ref} and x_{ext} are the absorbance of the solutions without and with the orange peel extract.

For measurements using our homebuilt photometer, the antioxidant activity is determined based on the voltage difference (Δv) recorded from the light-dependent resistor (LDR) sensor:

$$AA(\%) = \frac{\Delta v_{ref} - \Delta v_{ext}}{\Delta v_{ref}} \times 100\% \qquad (4)$$

where Δv_{ref} and Δv_{ext} are the voltage difference, corresponding to the absorption of the solutions without and with the orange peel extract.

3 Results and discussion

3.1 Visual Observation of DPPH Solutions

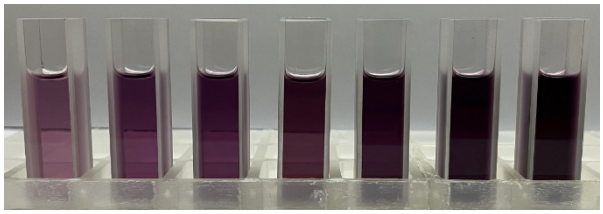

Fig. 1. Images of the diluted DPPH solutions with seven concentrations arranged sequentially from left to right: 0.10, 0.15, 0.20, 0.25, 0.30, 0.35, and 0.40 mM..

Figure 1 presents seven diluted DPPH solutions, each exhibiting a characteristic violet color. The intensity of the violet hue darkens as the concentration of DPPH increases, visually confirming that higher concentrations result in greater absorption of visible light. This observation aligns with the expected behavior of radical scavenging reactions, where higher molecular densities absorb more light, reducing transmission

3.2 Absorption Spectra of DPPH

Figure 2 illustrates the absorption spectra of the prepared DPPH solutions over the wavelength range of 400–700 nm, revealing a distinct absorption peak at 517 nm, characteristic of DPPH radical activity. Notably, all recorded spectral curves remain separate and well-defined, demonstrating that absorbance values increase consistently with higher DPPH concentrations. This confirms the expected relationship between concentration and optical absorption, where a greater number of radical molecules enhance light absorption, resulting in a darker solution appearance, as visually observed in figure 1.

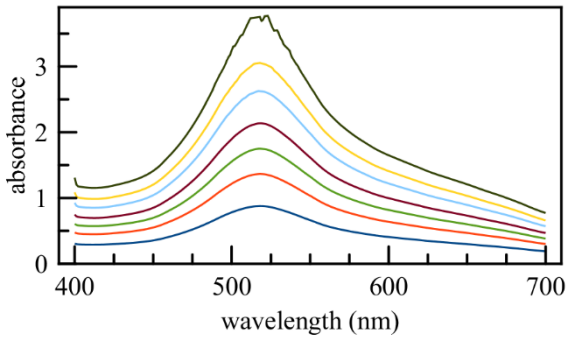

Fig. 2. Absorbance spectra of diluted DPPH solutions, with curves ordered from bottom to top, corresponding to concentrations of 0.10, 0.15, 0.20, 0.25, 0.30, 0.35, and 0.40 mM.

3.3 Calibration from Spectrophotometer

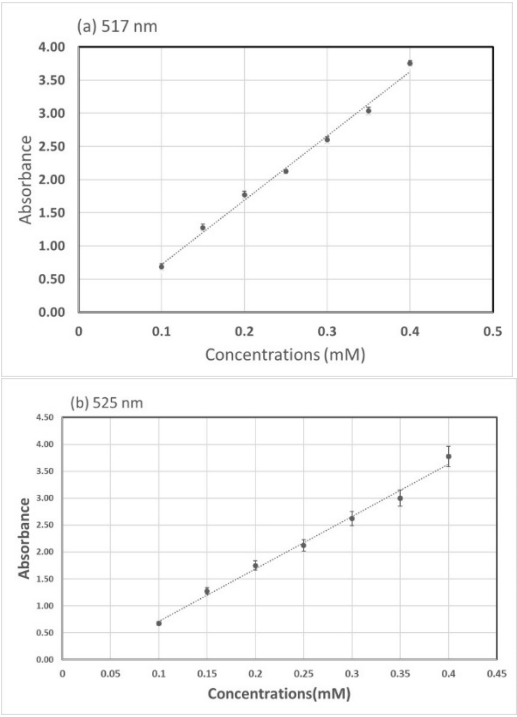

Fig. 3. Calibration curves of DPPH solutions at (a) 517 nm and (b) 525 nm, derived from spectrophotometric measurements. Circles represent the seven concentrations of the diluted DPPH solutions, plotted against the absorbance measured by the spectrophotometer. The lines denote the linear fits of the data.

The correlation between DPPH concentration and absorbance was analyzed using a linear regression model, formulated as Equation (1). Two distinct calibration equations were derived for measurements taken at 517 nm and 525 nm, expressed as:

$$y = 9.728\ x - 0.0255 \quad \text{(at 517 nm)} \qquad (5)$$

$$y = 9.731\ x - 0.258 \quad \text{(at 525 nm)} \qquad (6)$$

In both cases, the coefficient of determination (R^2) is exceptionally close to unity (0.9916 and 0.9921, respectively), indicating a strong fit to the linear regression, as illustrated in figure 3. These values suggest that both wavelengths are effective for DPPH analysis, though slight variations in slope (a) imply minor differences in light absorption efficiency.

3.4 Absorption of DPPH from Photometer

Table 1 shows the detailed measurements of the diluted DPPH solutions obtained from the homebuilt photometer. To minimize the electronic noise, each value of these digital voltages derived from an average of a thousand of raw data measured within a few seconds. The final values are rounded to two decimal places.

The blank voltages (v_0) of all seven measurements, in which a cuvette of 95% ethanal is placed in the photometer, are very similar. They are within a range of 951.46 – 951.93. The difference of the minimal and maximal values is only 0.47 which results in very small corresponding percentage difference of 0.049% [|951.46 – 951.93| / (951.46 + 951.93) ×2×100%]. This indicates that the homebuilt photometer works very reliable.

For the diluted DPPH solutions, the sample voltages (v) are lower than the blank voltage as the light is additionally absorbed by DPPH. When the DPPH concentration increases, the sample voltage (v) decreases. These results in the difference of the two voltages which taken as the sample absorption ($\Delta v = v_0 - v$) increases with the DPPH concentration.

Table 1. Absorption of diluted DPPH solutions measured by using the homebuilt photometer: the blank voltage (v_0), the sample voltage (v), and the absorption ($\Delta v = v_0 - v$).

DPPH (mM)	v_0	v	Δv
0.10	951.62	802.13	149.49
0.15	951.46	647.62	303.84
0.20	951.51	524.10	427.41
0.25	951.48	360.58	590.90
0.30	951.93	214.11	737.82
0.35	951.51	133.61	817.90
0.40	951.49	73.06	878.43

3.5 Calibration from Photometer

The digital voltage difference (Δv), obtained from the homebuilt photometer, exhibits a clear linear relationship with the DPPH concentration, similar to the absorbance behavior observed with the UV/Vis spectrophotometer. This reinforces the effectiveness of the LED-based detection system in quantifying DPPH concentration.

3.5.1 Overall Fitting

Figure 4(a) presents the calibration fitting results using equation (2). An overall fitting is performed using all collected data points, yielding the equation:

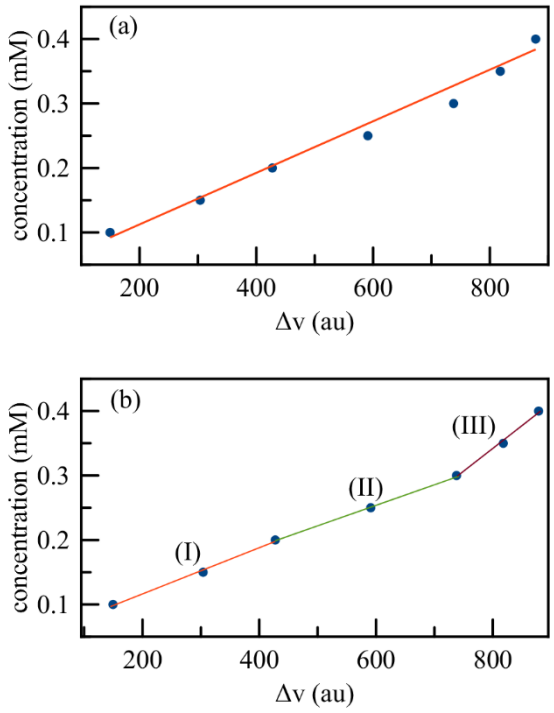

Fig. 4. Calibration curve of DPPH solutions obtained from measurements using the homebuilt photometer: (a) an overall fitting and (b) three piecewise fittings. Circles represent the seven concentrations of the diluted DPPH solutions, plotted against the digital voltage difference (Δv) measured by the photometer. The lines denote the linear fits of the data.

$$y = 3.90\times10^{-4}\,\Delta v + 0.0325 \qquad (7)$$

with the R^2 value of 0.9816. While this fitting confirms a strong correlation between DPPH concentration and voltage difference, the slightly lower R^2 value compared to those obtained from the spectrophotometric calibration (figure 3) suggests variations in measurement precision with the homebuilt photometer.

3.5.2 Piecewise Fitting

To enhance model accuracy and reduce residual errors, three piecewise fittings are performed for different concentration ranges of DPPH, as shown in figure 4(b):

range I: 0.1 mM ≤ y ≤ 0.2 mM

$$y = 3.58\times10^{-4}\,\Delta v + 0.0448 \qquad (8)$$

with the R^2 value of 0.99959,

range II: 0.2 mM ≤ y ≤ 0.3 mM

$$y = 3.22\times10^{-4}\,\Delta v + 0.0616 \qquad (9)$$

with the R^2 value of 0.9991, and

range III: 0.3 mM ≤ y ≤ 0.4 mM

$$y = 7.07\times10^{-4}\,\Delta v - 0.2234 \qquad (10)$$

with the R^2 value of 0.9936.

The R^2 values for all three piecewise fittings are very close to unity, confirming that segmented calibration models better fit the experimental data compared to the overall fitting approach. This refinement improves measurement precision by accounting for subtle variations in photometric response at different concentration levels.

3.6 Visual Observation of Mixtures

Figure 5 illustrates the visual transformation of DPPH solution color upon reaction with orange peel extract after being kept in darkness for 30 minutes. While the initial DPPH concentration remains at 0.4 mM, the volume of added extract varies, influencing the degree of radical scavenging activity. The progressive shift from violet to pale yellow is an observable indication of antioxidant action, where bioactive compounds in the extract neutralize DPPH radicals. The gradual color transition corresponds to the interaction between phenolic compounds and flavonoids from the orange peel extract with DPPH radicals, resulting in the observed reduction in light absorption.

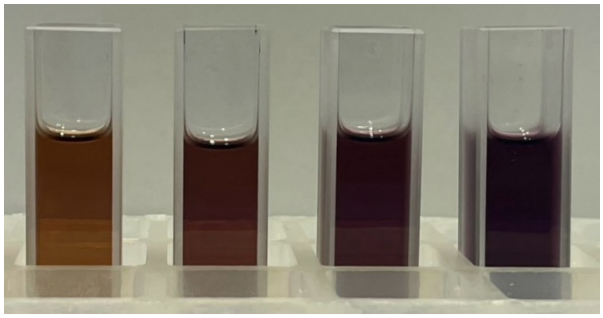

Fig. 5. Images of the mixtures containing DPPH and orange peel extract solutions, arranged sequentially from left to right with extract volumes of 0.6, 0.4, 0.2, and 0.0 ml.

3.7 Antioxidant Activity

Table 2. Antioxidant activity (AA) calculated from measurements by the spectrophotometer.

extract (ml)	AA (%)		
	517 nm	525 nm	average
0.0	0.0	0.0	0.0
0.2	24.8	26.5	25.7
0.4	48.5	50.1	49.3
0.6	64.3	66.0	65.2

The antioxidant activity (AA) calculated from absorption measurements in the spectrophotometer are summarized in table 2. AA increases with the added volume of the orange peel extract. Using equation 3, the measurements by the spectrophotometer with the wavelengths of 517 and 525 nm results very similar AA values with the difference about 1.6% - 1.7%. The average AA is also calculated and shown in table 2.

Table 3 shows AA values obtained from the measurements by the homebuilt photometer with the overall fitting and using equation 4. Similar to AA in table 2, it increases with the added volume of the extract. However, for each added volume, the AA value is quite different from those obtained from the spectrophotometer.

For quantitative comparison, we calculate the error by taking the AA value obtained from the spectrometer as reference. Even though for a given added volume of the extract the error depends on the reference (517nm, 525 nm, or average), the error increases with the added volume of the extract. from 0.2 to 0.6 ml, the error increases from 1.8% - 3.5% to 10.5% - 12.2%. We expect that the error comes from the fact that the single linear regression [figure4 (left)] does not fit well to the whole set data of the diluted DPPH solutions.

Table 3. Antioxidant activity (AA) calculated from measurements by the homebuilt photometer with overall fitting and the error in comparison to the results from the spectrometer.

extract (ml)	AA (%)	error (%) with ref.		
		517 nm	525 nm	average
0.0	0.0	0.0	0.0	0.0
0.2	23.0	1.8	3.5	2.7
0.4	55.9	7.4	5.8	6.6
0.6	76.5	12.2	10.5	11.3

Such error of AA obtained from the homebuilt photometer with overall fitting can be reduced when AA values are calculated based on the three piecewise fittings [figure4 (right)]. In this case, AA is not calculated from equation 4 but the equivalent DPPH concentration is calculated from Δv and the piecewise fitting before AA is calculated using equation (11) in which AA is defined as

$$AA(\%) = \frac{C_{ref} - C_{ext}}{C_{ref}} \times 100\% \qquad (11)$$

where C_{ref} and C_{ext} are the equivalent DPPH concentration without and with the orange peel extract.

Table 4. Antioxidant activity (AA) calculated from measurements by the homebuilt photometer with piecewise fittings and the error in comparison to the results from the spectrometer.

extract (ml)	AA (%)	error (%) with ref.		
		517 nm	525 nm	average
0.0	0.0	0.0	0.0	0.0
0.2	27.5	2.7	1.0	1.8
0.4	52.3	3.8	2.2	3.0
0.6	68.9	4.6	2.9	3.7

Table 4 shows AA values calculated from the piecewise fitting method. They are different from those calculated from the overall fitting method in table 3. When the added volume of the extract is increased from 0.2 - 0.6 ml, the error also increases from 1.0% - 2.7% to 2.9% - 4.6% but much less than the error from the overall fitting method in table 3.

4 Conclusion

Absorption-based measurements of antioxidant activity obtained from both the homebuilt photometer and the commercial spectrophotometer showed consistent results. In the case of the homebuilt photometer, the use of three piecewise linear fittings provided a more accurate representation of the absorption data than overall fitting. Moreover, the findings of this study further substantiate the applicability of LED-based detection systems for antioxidant analysis and highlight the advantages of refined calibration procedures in enhancing measurement accuracy. Future work may focus on further optimizing homebuilt photometers to improve precision, sensitivity, limits of detection, and other parameters that contribute to reducing variability in concentration estimation.

We thank the Department of Industrial Physics and Medical Instrumentation, King Mongkut's University of Technology North Bangkok and the Department of Physics, Kasetsart University for financial support.

References

1. V. Lobo, A. Patil, A. Phatak, N. Chandra, Free radicals, antioxidants, and functional foods: Impact on human health. Pharmacognosy Reviews **4**, 118-126 (2010).
2. N. Chandimali, S. G. Bak, E. H. Park, H. J. Lim, Y. S. Won, E. K. Kim, S. I. Park, S. J. Lee, Free radicals and their impact on health and antioxidant defenses: a review. Cell Death Discov. **11**, 19 (2025)
3. H. Sies, Oxidative stress: A concept in redox biology and medicine. Redox Biology **4**, 180-183 (2015).
4. G. Liguori, R. Ingrassia, A. C. Maio, Reactive oxygen species, toxicity, oxidative stress, and antioxidants. Arch. Toxicol. 97, 2737–2763 (2023).
5. M. Valko, C.J. Rhodes, J. Moncol, M. Izakovic, Free radicals, metals and antioxidants in oxidative stress-induced cancer. Chem. Biol. Interact. **160**, 1-40 (2006).
6. L. Di Meo, C. Natalucci, S. Percario, et al., Oxidative stress and metabolic disorders: relevance and therapeutic perspectives. Front. Nutr. **9**, 994309 (2022)
7. G. Alamdari, M. Mohseni, S. Sadeghi, et al., Free radicals, antioxidants and functional foods: impact on human health. J. Med. Food **14**, 795–802 (2011).
8. S. Smith, J. Jones, and R. Taylor, Free radicals and their impact on health and antioxidant defenses. Cell Death Discov. **10**, 1234 (2024)
9. M. P. Kahkonen, A. T. Hopia, H. J. Vuorela, Antioxidant activity of plant extracts containing phenolic compounds. J. Agric. Food Chem. **47**, 3954-3962 (1999)
10. M. M. Rahaman, R. Hossain, J. Herrera-Bravo, et al., Natural antioxidants from some fruits, seeds,

foods, natural products, and associated health benefits: An update. Food Sci. Nutr. **11**, 1657–1670 (2023).

11. I. N. Monroy-García, S. Torres-Romero, L. D. Castro-Ochoa, A. Mendoza-Acosta, E. Viveros-Valdez, F. Ayala-Zavala, Bioactive compounds from marine macroalgae: A natural defense against oxidative stress-related diseases. Stresses **5**, 22 (2025)
12. F. Menaa, U. Wijesinghe, G. Thiripuranathar, et al., Marine algae-derived bioactive compounds: a new wave of nanodrugs? Mar. Drugs **19**, 484 (2021)
13. S. Ghosh, T. Sarkar, S. Pati, et al., Novel bioactive compounds from marine sources as a tool for functional food development. Front. Mar. Sci. **9**, 1–28 (2022)
14. R. L. Prior, X. Wu, K. Schaich, Standardized methods for the determination of antioxidant capacity in food and dietary supplements. J. Agric. Food Chem. **53**, 4290-4302 (2005)
15. C. A. Rice-Evans, N. J. Miller, G. Paganga, Structure-antioxidant activity relationships of flavonoids and phenolic acids. Free Radic. Biol. Med. **20**, 933-956 (1996)
16. W. Brand-Williams, M. E. Cuvelier, C. Berset, Use of a free radical method to evaluate antioxidant activity. LWT - Food Science and Technology **28**, 25-30 (1995)
17. K. Benzie, J. Strain, Ferric reducing/antioxidant power assay: Direct measure of total antioxidant capacity. Methods in Enzymology. **299**, 15-27 (1999)
18. A. Bocco, M. E. Cuvelier, H. Richard, C. Berset, Antioxidant activity and phenolic composition of citrus peel and seed extracts. J. Agric. Food Chem. **46**, 2123-2129 (1998).
19. P. Kolesnichenko, A. Eriksson, L. Lindh, D. Zigmantas, J. Uhlig, Viking spectrophotometer: a home-built, simple, and cost-efficient absorption and fluorescence spectrophotometer for education in chemistry. J. Chem. Educ. **100**, 1561–1567 (2023)
20. V. R. Pereira, B. S. Hosker, Low-cost (<€5), open-source, potential alternative to commercial spectrophotometers. PLoS Biol. **17**, e3000321 (2019)
21. A. B. D. Nandiyanto, R. Zaen, R. Oktiani, et al., Techno-economic feasibility study of low-cost and portable home-made spectrophotometer for analyzing solution concentration. J. Eng. Sci. Technol. **14**, 599–609 (2019)
22. H.-Y. Chen, H.-M. Nieh, M.-F. Yang, et al., Implementation of a low-cost automated LED photometer for enzymatic reaction detection to teach basic bioelectronics technologies in vocational high schools. IEEE Trans. Educ. **59**, 194–201 (2016)
23. E. M. Paiva, J. Rohwedder, C. Pasquini, C. Pereira, Method for building a portable near infrared photometer based on LEDs and interference filters chosen by a spectral variable selection algorithm. Microchem. J. **146**, 842–849 (2019)
24. R. Shi, C. Wang, M. Zhu, C. Xie, W. Cui, Q. Zhou, A smartphone-assisted colorimetric paper sensor based on MnO_2 nanozymes for rapid evaluation of total antioxidant capacity in foods. Microchim. Acta **192**, 414 (2025)
25. D. Calabria, M. Guardigli, P. Severi, I. Trozzi, A. Pace, S. Cinti, M. Zangheri, M. Mirasoli, A smartphone-based chemosensor to evaluate antioxidants in agri-food matrices by in situ AuNP formation. Sensors **21**, 5432 (2021)
26. Z. Ying, L. Qiao, B. Liu, L. Gao, P. Zhang, Development of a microfluidic wearable electrochemical sensor for the non-invasive monitoring of oxidative stress biomarkers in human sweat. Biosens. Bioelectron. **261**, 116502 (2024)
27. R. K. Saini, A. Ranjit, K. Sharma, P. Parchuri, X. Shang, K. Gowda, Y.-S. Keum, Bioactive compounds of citrus fruits: A review of composition and health benefits of carotenoids, flavonoids, limonoids, and terpenes. Antioxidants **11**, 239 (2022)
28. B. Singh, J. P. Singh, A. Kaur, N. Singh, Phenolic composition, antioxidant potential and health benefits of citrus peel. *Food Res. Int.* **132**, 109114 (2020)
29. J. H. Park, M. Lee, E. Park, Antioxidant activity of orange flesh and peel extracted with various solvents. Prev. Nutr. Food Sci. **19**, 291-298 (2014)
30. S. Jaiswal, S. S. Gaur, Orange peel and skin health: An exploratory study on potential benefits. J. Food Chem. Nanotechnol. **9**, S91-S99 (2023)
31. A. El-Sayed, M. Shehata, N. Abdel-Haleem, et al., Bioactive preservative nano-packaging films based on orange peel waste extracts: antioxidant and antimicrobial efficacy. Bioresour. Bioprocess. **12**, 1–18 (2025)
32. D. Gabrić, M. Kurek, M. Ščetar, M. Brnčić, K. Galić, Characterization of synthetic polymer coated with biopolymer layer with natural orange peel extract aimed for food packaging. Polymers **15**, 2569 (2023)